A double-layer Optimization Framework for the Design and Operation of Thermal Energy Storages in renewable-based Virtual Power Plants

Simone Peccolo[a], Lorenzo Gasperin[b], Andrea Parelli[c], Anna Stoppato[d] and Alberto Benanto[e]

University of Padova, Department of Industrial Engineering (DII), Padova, Italy

[a] *simone.peccolo@phd.unipd.it*

[b] *lorenzo.gasperin.1@phd.unipd.it*

[c] *andrea.parelli@studenti.unipd.it*

[d] *anna.stoppato@unipd.it*

[e] *alberto.benato@unipd.it, CA*

Abstract:

Our society is undergoing an energy transition that promotes increasing deployment of renewable energy sources to reduce greenhouse gas emissions. However, the growing share of intermittent renewables intensifies the mismatch between energy production and demand. To address this challenge, it is essential to develop technologies capable of storing surplus renewable energy for later use. Among thermal energy storage solutions, Carnot Batteries - and in particular Integrated Energy Storage Systems (I-ESS) - offer a promising alternative due to their competitive cost, absence of geographical constraints, and compatibility with existing power plants. The core element of I-ESS is a sensible heat storage unit designed as a packed bed employing safe, non-toxic, and non-flammable solid materials. Despite the increasing interest in these systems, current literature lacks comprehensive methodologies that simultaneously address the optimal design and operational management of thermal energy storage within complex multi-energy networks. To fill this gap, we propose a double-layer optimization framework for the integrated design and operation of a multi-energy Virtual Power Plant (VPP) centered on an I-ESS. An external metaheuristic layer based on Particle Swarm Optimization determines the optimal sizing of VPP components, while an internal Mixed-Integer Linear Programming model computes the cost-optimal hourly dispatch and energy flow management. This structure enables tractable optimization over year-long scenarios with hourly resolution. The methodology is applied to realistic Virtual Power Plant configurations comprising a photovoltaic power generation system, the electrical grid, end users, a natural gas boiler, an Integrated Energy Storage System (I-ESS), and auxiliary storage devices for combined electricity and heat supply. Results show that the proposed framework increases renewable energy utilization and reduces grid dependence through coordinated management of generation and storage assets. For the considered case study, 39.7% of the electrical demand is supplied by the photovoltaic system, 36.9% by the I-ESS, and the remaining 23.4% by the grid. In addition, the secondary thermal storage device enables approximately 30% of the thermal demand to be met, thereby reducing natural gas consumption. Overall, the framework provides a scalable and robust approach for integrating thermal energy storage into complex multi-energy networks.

Keywords:

Thermal Energy Storage; Renewable Energy Sources Integration; Integrated Energy Storage System; Optimization; Particle Swarm Optimization; Mixed Integer Linear Programming.

1. Introduction

The global transition toward low-carbon energy systems has significantly increased the penetration of intermittent renewable energy sources (RES), such as solar and wind. According to the Interna-

tional Energy Agency, in the next decades there will be an increase of the installations of RES based power production plants. The global RES generation will rise annually o by around 1050 TWh to the end of this decade. Solar and wind installations are expected to continue to increase of more than 600 TWh annually to the end of 2030, as reported in the "Electrictiy 2026" report [1]. The RES like wind and solar are characterized by fluctuations during the days and along the year, due to their intrinsic variability and unpredictable behaviour. This shift towards RES creates substantial imbalances between energy generation and demand, necessitating the integration of robust energy storage technologies to maintain grid stability [2, 3]. While established solutions like Pumped Hydro Storage (PHS) and Compressed Air Energy Storage (CAES) are widely used, they are often limited by specific geographical requirements and high investment costs [4]. In this context, Carnot Batteries (CBs), specifically Pumped Thermal Energy Storage (PTES), emerge as promising alternatives due to their high energy density, site independence, and long lifespan [5, 6]. Carnot Batteries are used to accumulate the surplus of the electricity production in the form of heat inside storage device and to exploit it when necessary, through the reconversion of the heat in electrical energy. The Integrated Energy Storage System (I-ESS) was developed by the Authors starting from the concept of PTES [7, 8]. This accumulation device stores the surplus of electrical energy in the form of sensible heat in a high-temperature storage tank with a packed-bed arrangement. During the reconversion of heat in electricity, the I-ESS operates an air cycle that replies to the behaviour of a gas turbine. The simplicity of I-ESS coupled with good efficiency and long lifespan and not requiring any geographical constraint make it a valid and alternative solution. Until now, the literature deeply investigated the thermodynamics models of these devices, such as the TES-PD model [9, 10], but often lacks comprehensive optimization frameworks that simultaneously address the sizing and operational management of complex multi-energy systems integrating thermal storage under full-year hourly simulations. Moreover, many existing studies rely on representative days (such as [11] and [12]), which may fail to capture the long-term variability of weather-dependent generation and multi-vector demands. To bridge this gap, this study proposes a double-layer optimization framework combining a Particle Swarm Optimization (PSO) for component sizing and a Mixed-Integer Linear Programming (MILP) for cost-optimal hourly dispatch over a full-year horizon. The framework is applied to a residential neighbourhood in Northern Italy, integrating a photovoltaic plant, an Integrated Energy Storage System (I-ESS) and a secondary thermal storage to maximize economic performance. The proposed methodology leverages a hybrid PSO-MILP framework to navigate the complex design space of system component sizing. By employing Particle Swarm Optimization (PSO) as the outer metaheuristic, the model facilitates high-fidelity representation of system devices. For every configuration identified by the PSO, an internal Mixed-Integer Linear Programming (MILP) model determines the optimal hourly dispatch strategy over a one-year horizon. This large-scale optimization, comprising hundreds of thousands of variables, is processed through the Gurobi commercial solver [13] to maximize total economic benefits. This approach marks a significant advancement from conventional methods, offering a balance between modelling accuracy, real-world constraint satisfaction, and computational efficiency. The rest of the paper is organized as follow: in Section 2.1. the innovative bi-level framework and its functioning will be described, while in Section 2.2. the energy network will be presented. Lastly Section 3. will analyse the major results obtained from the numerical simulations.

2. Methods

2.1. The double-layer optimization framework

The study proposes a hybrid double-layer optimization framework designed to address the complexity of multi-energy systems by integrating a Particle Swarm Optimization (PSO) algorithm at the outer level and a Mixed-Integer Linear Programming (MILP) model at the inner level. This architecture decouples the decision variables into two coordinated layers: the outer PSO layer identifies the optimal sizing of the system components, while the inner MILP layer determines the cost-optimal hourly

dispatch and management of energy flows for each candidate configuration over a full-year horizon. This decoupling allows the inner MILP model to incorporate realistic operational constraints and part-load behaviours while maintaining a linear formulation, thereby avoiding the high computational complexity associated with non-linear models. Moreover the exploitation of a MILP formulations allows for simulating a year-long scenario with hourly resolution, involving a high number of variables and constraints.

The PSO algorithm treats each particle in the swarm as a candidate solution in an n-dimensional space, where each dimension corresponds to a sizing optimization variable. The position of each particle p_i is iteratively updated based on a velocity vector V_i that balances three components: inertia, individual memory (the best solution found by that particle, $p_{best,i}$), and collective learning (the best solution found by the entire swarm, g_{best}), according to Equation 1 and Equation 2.

$$p_i(t) = p_i(t-1) + V_i(t) \tag{1}$$

$$V_i(t) = \omega \cdot V_i(t) + r_1 \cdot c_1 \cdot (p_{best,i} - p_i) + r_2 \cdot c_2 \cdot (g_{best} - p_i) \tag{2}$$

In Equation 2, ω represents the inertia coefficient, c_1 and c_2 are the cognitive and social acceleration coefficients and r_1 and r_2 are two coefficients of uniformly distributed random numbers in the interval [0 1].

To optimize the search process, the framework employs several advanced strategies. The inertia coefficient (ω) and the cognitive and social acceleration coefficients (c_1, c_2) vary linearly across iterations, accordingly to Equations 3, 4 and 5.

$$\omega(t) = \omega_{max} - (\omega_{max} - \omega_{min}) \cdot t/t_{max} \tag{3}$$

$$c_1(t) = c_{1,max} - (c_{1,max} - c_{1,min}) \cdot t/t_{max} \tag{4}$$

$$c_2(t) = c_{2,max} - (c_{2,max} - c_{2,min}) \cdot t/t_{max} \tag{5}$$

During the initial exploration phase, high ω and c_1 values are used to promote a broad search of the design space. In the final exploitation phases, c_2 is maximized while ω and c_1 are decreased to encourage convergence toward the global optimum. To ensure a well-dispersed and representative initial sampling of the multidimensional search space, Latin Hypercube Sampling (LHS) is applied to the optimization variables. Lastly, to reduce computational time, the algorithm monitors the global best solution (g_{best}); if no significant improvement is found over a set number of iterations, the process terminates early.

As mentioned, the energy management and dispatch problem is formulated as a MILP model solved using the Gurobi solver [13]. A key feature of the proposed framework is the implementation of a dynamic MIPgap strategy synchronized with the PSO's progress. During the initial PSO exploration (0-40% of iterations), a higher MIPgap (up to 5%) is imposed to accelerate the solver's convergence when particles are exploring potentially suboptimal regions. As the PSO transitions to exploitation (75-100% of iterations), the MIPgap is tightened to 0.5%. Since the solver is operating within a near-optimal domain at this stage, the increased precision does not significantly inflate overall calculation times, allowing for a precise final convergence to the global optimum. The adoption of an internal MILP algorithm allows for solving a computationally complex problem, characterized for a high number of variables, deriving from the necessity of simulate an entire year with hurly resolution.

Through the proposed double-layer framework it is possible to accurately describe the various component of the energy system, including their operational limits, while maintaining good computational time and performance.

2.2. The energy network

Before analysing the proposed case study and the energy system, it is fundamental to understand the functioning of the Integrated Energy Storage System (I-ESS). A scheme of the charging and discharging process of the system is reported in Figure 1.

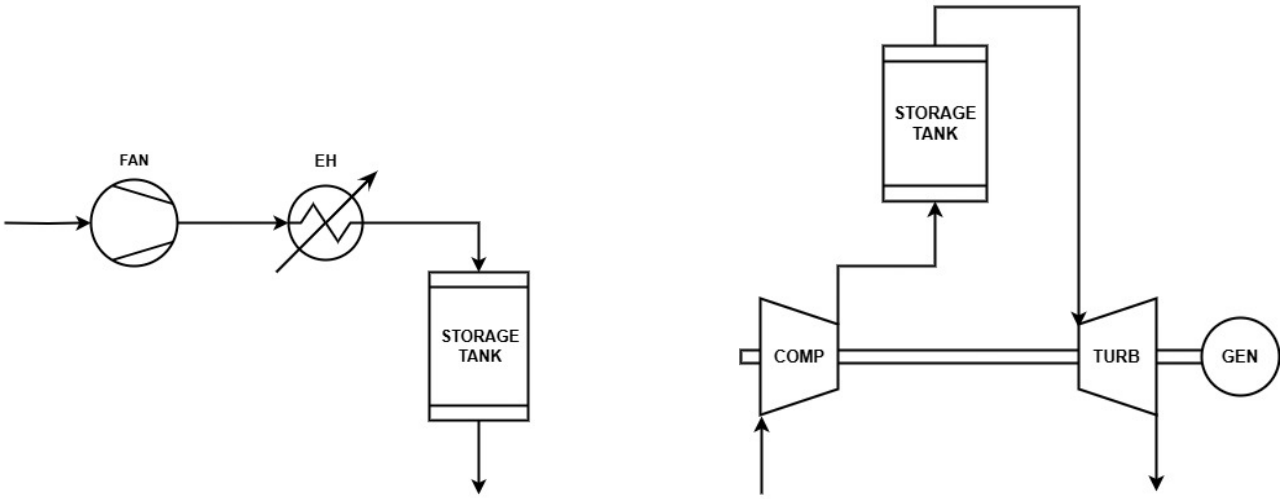

(a) Charge (b) Discharge

Figure 1: Scheme of the I-ESS for the charge and the discharge.

During the charging process, the air is withdrawn from the external environment through a fan and is sent to an electric heater where its temperature is increased at the desired value (1000 °C). The hot air, passing through the packed-bed storage tank, releases its energy that is accumulated inside the storage medium (Alumina). During the discharging process, the cycle is operated as a gas turbine in which the combustion chamber has been replaced by the thermal storage tank. In both the processes, the air exiting the storage device and released to the external environment still have a certain energy content that can be exploited for providing heat for industrial processes or for space heating. In this work, it was decided to recover this energy through the usage of a secondary thermal energy storage tank, using diathermal oil as storage medium (Therminol 68 [14]). The air coming from the I-ESS exchange heat with the storage material through the usage of heat exchangers. When needed, the energy can be extracted from the storage tank using water to supply thermal energy to the users. Downstream these considerations, the energy network considered as case study in this work comprises a photovoltaic (PV) facility, the I-ESS, the electrical grid (G) and the secondary thermal energy storage (V2), a system of natural gas boilers (B) and a system of users (U). The entire network need to be managed to fulfil the user requirements in term of electrical and thermal demands. The thermal energy storage systems and the photovoltaic power plant are treated as a Virtual Power Plant (VPP), aimed in supplying energy to the system of users during the whole year. A schematic view of the VPP considered in this work is reported in Figure 2, highlighting the possible energy exchanges between the various components of the network. The PV plant can exchange energy directly to the users or can deliver it to the I-ESS for accumulating the surplus of electricity. Otherwise, the photovoltaic facility can send the energy not used to the electrical grid. Similarly, the energy stored in the I-ESS can be exploited to produce electricity to fulfil the electrical demand of the users or can be sold to the grid. The I-ESS can be also charged through the energy withdrawn from the electrical grid. As previously said, the energy content of the air not exploited during the accumulation and discharging processes, is accumulated in the secondary thermal energy storage, as previously mentioned. The energy accumulated can be used for supplying heat to the users. When the energy is not enough to meet the users' thermal requirements it is necessary to exploit the system of natural gas boilers.

To accurately estimate the behaviour of the VPP, it is necessary to model the various components of

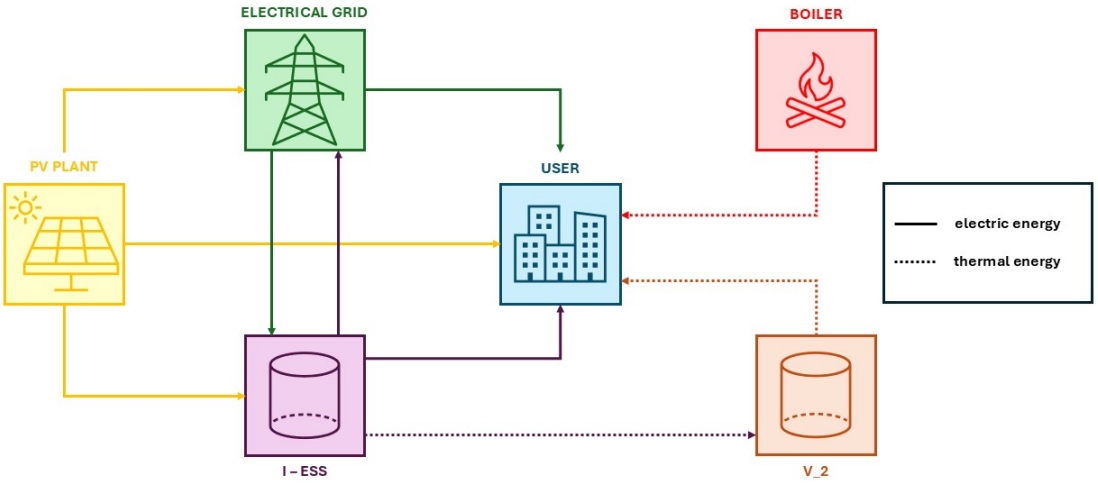

Figure 2: The energy network with the interconnections between its components.

the network and characterized the devices considering real-world data. Accordingly, the PV plant has been characterized considering hourly values of the irradiance derived from the PV-GIS database [15]. The selected location for the system is in the North of Italy, more precisely in the province of Rovigo.

The purchase price of the electrical energy is derived from the Gestore Mercati Energetici (GME) website [16], considering the Single National Price (Prezzo Unico Nazionale - PUN) with hourly resolution. From the GME we can also obtain the value of the price of the natural gas on a daily basis. The electrical energy produced by the PV facility and the I-ESS can sold to the electrical grid at a lower price, assumed equal to the 10 % of the corresponding price of the PUN, maintaining its variability along the year.

The thermal and electrical demands of the users are obtained considering data available in literature [17]. The demands present a hourly and seasonal variability, accurately describing the user requirements along the year. Different typologies of users has been considered in the work, aiming at replicating a variegated set of users. In this work two different configuration are investigated: the first one refers to a typical Italian neighbourhood located in the North side of the Country, while the second configuration accounts for a set of users belonging to the tertiary sector The number and the type of the users considered are reported in the following Table 1 for the two considered scenarios.

Table 1: Number and type of users considered in the first scenario.

User type	**Number**	
	Scenario 1	**Scenario 2**
Single residential house	350	-
Residential building	20	-
Office building	7	10
Shopping centre	-	10
Hospital	-	1
Hotel	-	2
Sports centre	-	1

The numerical modelling of the Integrated Energy Storage System has been previously investigated by the Authors [10, 18]. Starting from the TES-PD model, the Authors derived three curves that are implemented in the double-layer framework to characterize the I-ESS and its behaviour [19]. The

first curve, reported in Figure 3, represents the maximum and the minimum energy levels that can be reached for a certain volume of the I-ESS. Figure 4a and Figure 4b depicts the evolution of the charging and discharging efficiency as a function of the State of Charge (SOC) of the I-ESS. During the charge, when the SOC reaches high values, the efficiency suddenly drops, due to the reduction of the temperature difference between the hot air and the storage medium, that strongly penalizes the heat transfer. The same effect is observable during the discharging phase, when the SOC reaches lower values: similarly, the heat transfer is penalized by the reduction of the temperature difference between the heat transfer fluid and the storage material, coupled with the limits associated to the correct functioning of the turbomachinery.

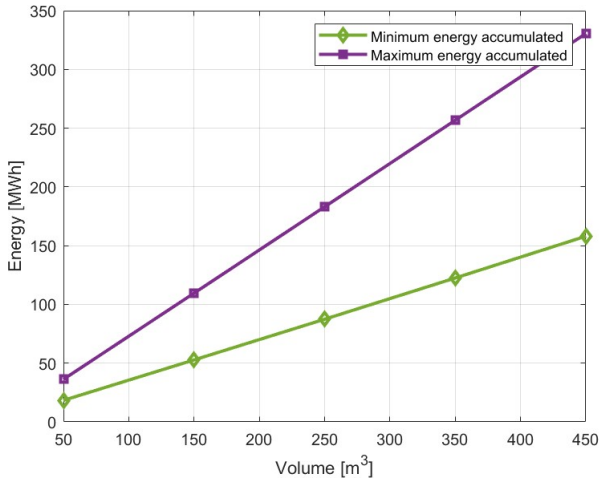

Figure 3: Maximum and minimum energy that can be accumulated for a certain volume of the I-ESS storage tank.

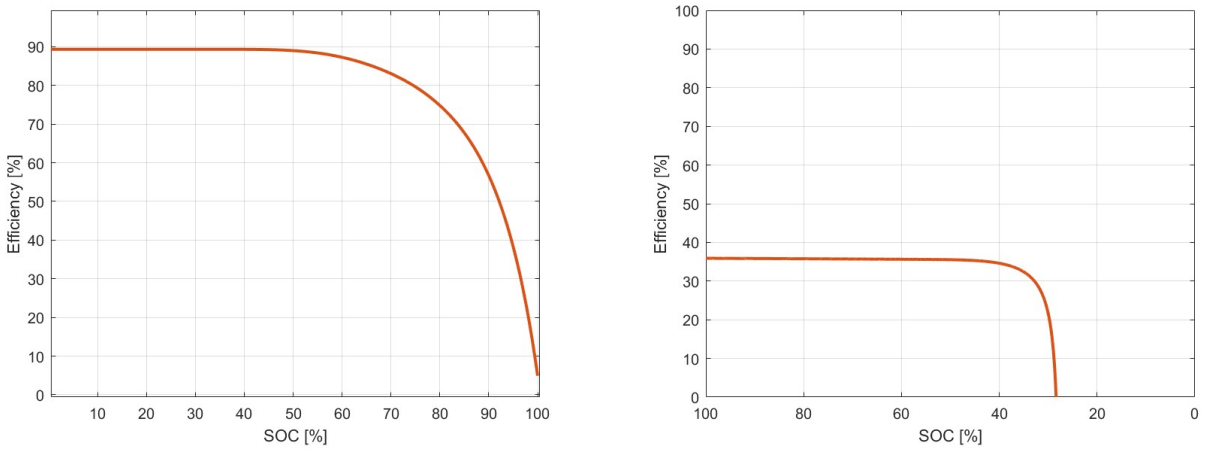

(a) Charge

(b) Discharge

Figure 4: Charging and discharging efficiencies as a function of the SOC of the I-ESS.

In the modelling of the I-ESS implemented in the double-layer optimization framework, the operational limits of the turbomachines are included as well: they can be operated between the 30 % and the 110 % with respect to the nominal power.

The VPP and its modelling have been included in the optimization framework through boundaries and constraints between the optimization variables. It is important to observe that the usage of the double-layer framework permits to introduce complex relationships between the variables. The usage of Piecwise Linear (PWL) constraints allows modelling the operational limits of the I-ESS in terms of maximum and minimum achievable energy level of the SOC as a function of the volume, while

binary variables have been chosen for the modelling of the non-simultaneous charge and discharge of the I-ESS. In addition to these, the use of the Indicator Constraints permits to describe the partial load functioning of the turbomachinery of the I-ESS for both the charging and the discharging phases.
The scope of the double-layer framework is to simultaneously define the sizing of the main components of the VPP and its hourly management. Accordingly, the optimization variables for the external PSO algorithm regards the sizes of the components, and in particular they are the area of the PV plant, (A), the nominal powers of the charging and discharging process of the I-ESS (respectively, P_{ch} and P_{dis}), its volume (V_1) and the volume of the secondary thermal energy storage (V_2). The role of the internal MILP regards the optimal hourly dispatch of the energy between the various components. This is done on an economical prospective, comparing the Net Present Value (NPV) of the optimized configuration and the NPV of the baseline one. This configuration is the one in which the system of users only fulfil its requirements through the electrical grid and the system of natural gas boilers. Thus the difference of the two NPVs has been chosen as the optimization variable of the problem. Equation 6 reports the calculation of the NPV.

$$NPV = -I_0 \cdot \sum_{t=1}^{year} \frac{CF}{(1+r)^t} \tag{6}$$

The term I_0 refers to the initial capital expenditure, while CF are the cash flows for the considered year, calculated considering the cost of the energy purchased from the electrical grid and the natural gas used in the system of boilers and the revenues deriving from the sold of electricity to the grid, from the PV plant and the I-ESS. Lastly, r is the discount factor. It is important to note that since the system of natural gas boilers is present in both the configurations, it was decided to not include its cost in the computation of the NPV. The costs of the various components are reported in Table 2. The operation and maintenance (O&M) costs are assumed to be equal to 5 % of the investment of each component

Table 2: Components and their specific costs.

Component	**Variable**	**Value**	**Unit**
PV plant	A	150	€/m^2
I-ESS, Volume	V_1	7180	€/m^3
I-ESS, Charge power	P_{ch}	337	€/kW
I-ESS, Discharge power	P_{dis}	307	€/kW
Volume V2	V_2	2310	€/m^3

3. Results and discussion

Before analysing the results of the optimization process, it was necessary to perform a sensitivity analysis on the number of particles and the maximum number of iterations of the PSO. These parameters are of central importance, since they affect the quality of the results of the process as well as the computational time. Several configurations have been testes, and the one that leaded to good results, maintaining good computational time is the one with 10 particles and 120 maximum number of iterations.
The results of the optimization process for the two configurations studied are grouped in Table 3, in terms of sizes of the components of the VPP. The results present some differences even if in both the cases there is a clear advantage in installing the PV plant, the I-ESS and the secondary thermal energy storage device. With respect to the baseline configuration in which the users withdrawn electricity and thermal energy exploiting the electrical grid and the system of boilers, both the optimized configurations represents a lower costs, leading to advantages for the users. At the same time, there are some differences between the two scenarios. The second scenario presents a higher surface for the installation of the photovoltaic power plant. Similarly, the volume of the I-ESS is increased as

well, even if the charging and discharging rated powers present only a marginal increase. The secondary thermal energy storage instead presented a large increase. The fundamental difference lies in the varying electrical and thermal load curves. The tertiary sector scenario includes users characterized by more constant consumption throughout the year. The electrical demand in Winter is higher compared to residential users, whereas summer consumption is lower. During the winter, the thermal consumption is effectively halved compared to the residential case; however, it is higher during the summer months.
In the Scenario 2, the higher demand during the central hours of the day permits to better exploit the photovoltaic production. In fact, the optimized configuration presents a greater surface A. During the summer, the increased thermal demand in the Scenario 2, justifies a larger value of the secondary thermal energy storage, that can be used for better fulfilling the users requirements in terms of thermal energy.

Table 3: Results in terms of sizes of the optimized configuration of the VPP.

Component	**Variable**	**Value**		**Unit**
		Scenario 1	**Scenario 2**	
PV plant	A	40270	53843	m^2
I-ESS, Volume	V_1	80	92	m^3
I-ESS, Charge power	P_{ch}	5140	5713	kW
I-ESS, Disharge power	P_{dis}	1380	1638	kW
Volume V2	V_2	10	19	m^3

From the comparison of the share of energy coming from the different devices of the VPP for the electrical and thermal demands, it is possible to observe some differences between the two scenarios. Figure 5 reports the shares in absolute terms for the electrical demand. The energy demanded along the year presents several differences due to the different typologies of users considered in the two scenarios. The users of the tertiary sector are characterized by a more constant electricity demand along the year, while the users belonging to the Scenario 1 present higher fluctuations.

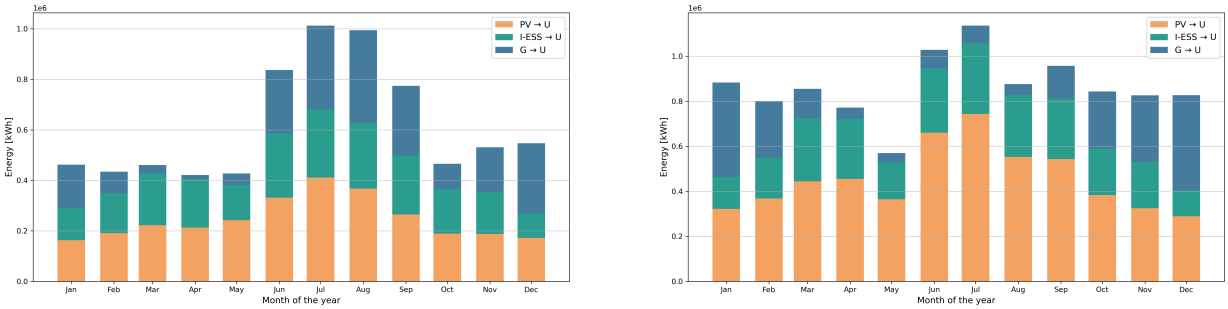

(a) Scenario 1

(b) Scenario 2

Figure 5: Comparison of the share of electrical energy for fulfilling the electrical demand of the users for the two considered scenarios.

Figure 6 reports the same results, but in relative terms. For The Scenario 1 the optimized configuration was able to cover the electrical demand for around 40% from the PV plant, the 31% derives from the I-ESS and the remaining 29% is withdrawn from the electrical grid. A different trend is obtained in the Scenario 2, where the photovoltaic facility is responsible for covering 53% while the I-ESS of about the 26%. The electrical grid is used to covering the remaining 21%. With respect to the Scenario 1 the renewable sources are better exploited, also due to the larger surface of the PV plant. The share of the I-ESS is more or less the same in both the cases. Moreover, the more constant electrical demand of the Scenario 2 along the year is beneficial in particular during the Summer, where the photovoltaic plant is exploited in a highly-efficient way, minimizing the consumption of electricity from the electrical grid.

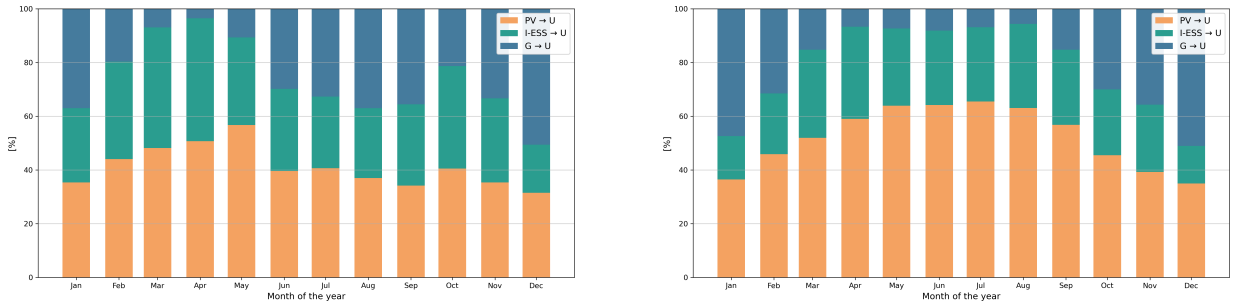

(a) Scenario 1 (b) Scenario 2

Figure 6: Comparison of the relative share of electrical energy for fulfilling the electrical demand of the users for the two considered scenarios.

In Figure 7 and Figure 8 are reported the same charts for the thermal demand. In the Scenario 1, the introduction of the secondary thermal energy storage system supplied to the system of users about 22% of the thermal demand. For the Scenario 2, the V2 supplied instead around 47% of the demand. It is important to note that the thermal demand in absolute terms is lower for the users belonging to the tertiary sector and, at the same time, is better distributed along the seasons with respect to the Scenario 1, with solely residential users.

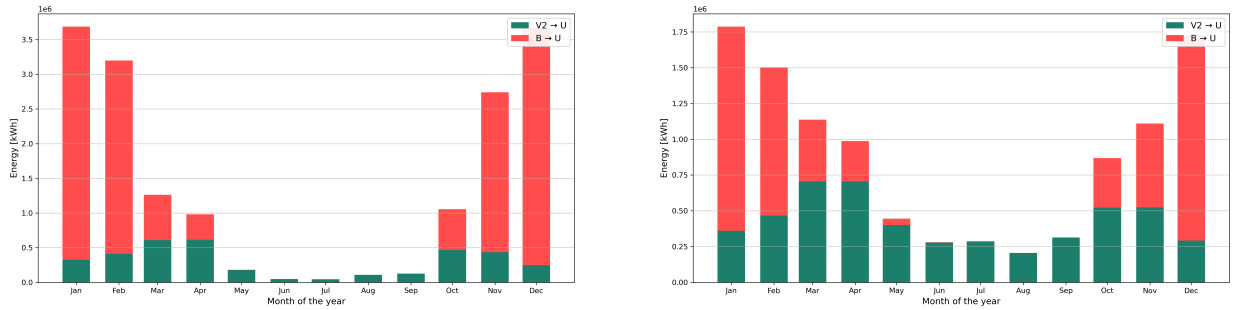

(a) Scenario 1 (b) Scenario 2

Figure 7: Share of thermal energy for fulfilling the thermal demand of the users for the two considered scenarios.

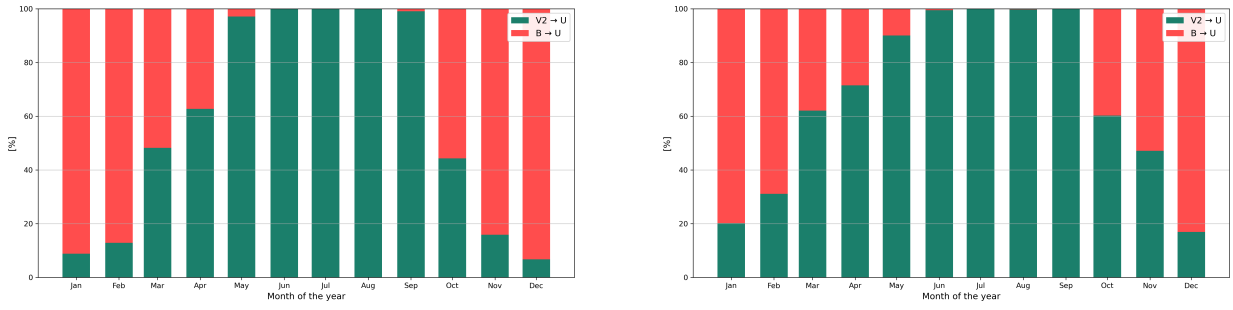

(a) Scenario 1 (b) Scenario 2

Figure 8: Share of thermal energy for fulfilling the thermal demand of the users for the two considered scenarios, in relative terms.

Another interesting consideration regards how the I-ESS is exploited for different days during the year. Figure 9 shows the SOC for different hours of the day and for different days along the year for the Scenario 1, but similar results have been obtained even for the Scenario 2. During the central hors of the days the SOC assumes generally higher values since the surplus of production from the PV plant is used to charge the I-ESS. During the night and in the early morning the SOC decreases, meaning

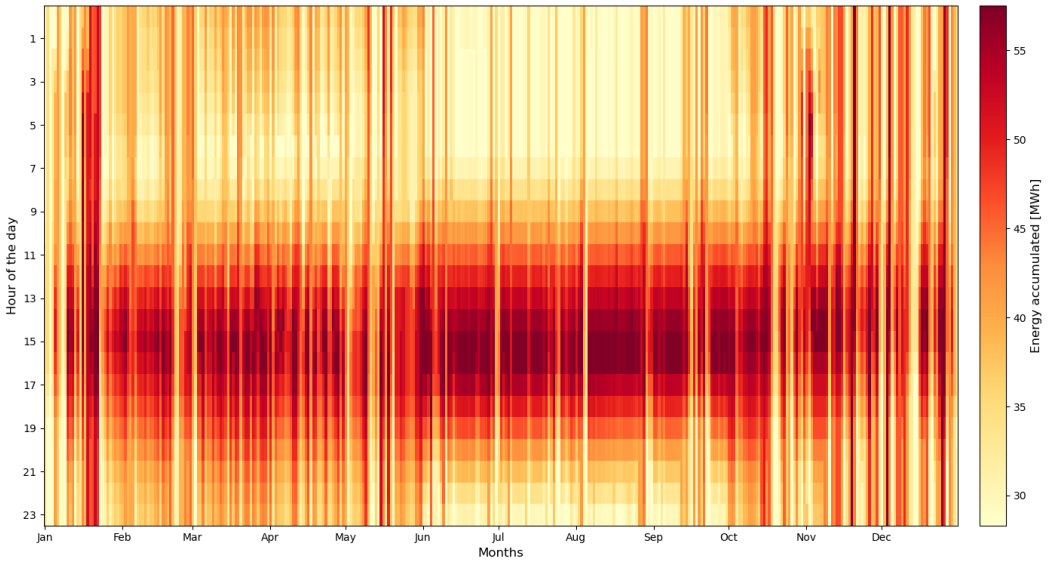

Figure 9: State of charge of the I-ESS for different hours of the day and for different days along the year.

the the I-ESS is used for supplying energy to the users. During the night, not only the PV plant is not producing electricity but also the PUN assumes higher values. It is clear that the implementation of the I-ESS permits to reduce the money expenditure for covering the electrical demand during these hours. Considering the variability of the SOC for different seasons, we observe that it assumes higher values during the summer, seen the greater production of electrical energy by the photovoltaic facility.

4. Conclusions

The proposed double-layer framework, which combines an external Particle Swarm Optimization (PSO) layer for sizing with an internal Mixed-Integer Linear Programming (MILP) model for hourly dispatch, proved to be a robust and scalable tool. This architecture effectively handles the complexity of multi-energy networks over a full-year horizon while maintaining computational efficiency through strategies like dynamic MIPgap synchronization. The framework successfully increased renewable energy utilization and significantly reduced dependence on the electrical grid through coordinated management of generation and storage assets. By effectively coordinating renewable generation and thermal storage, the system achieved significant increases in energy independence, reducing grid reliance. The framework demonstrated high economic viability through peak shaving and strategic energy discharge during high-price periods, consistently yielding lower operational costs and savings compared to baseline configurations. Furthermore, the integration of secondary thermal storage successfully displaced a substantial portion of natural gas consumption for heating, particularly in the tertiary sector where load profiles align well with solar production. These results lead to the conclusion that such an optimized multi-energy approach offers a safe, geographically flexible, and computationally efficient solution for modern energy transitions across various sectors.

References

[1] International Energy Agency. *Electricity 2026*. Tech. rep. License: CC BY 4.0. Paris: IEA, 2026.

[2] Zakariya Dalala et al. “Increased renewable energy penetration in national electrical grids constraints and solutions”. In: *Energy* 246 (2022), p. 123361.

[3] Marc Beaudin et al. “Energy storage for mitigating the variability of renewable electricity sources: An updated review”. In: *Energy for sustainable development* 14.4 (2010), pp. 302–314.

[4] Alberto Benato and Anna Stoppato. “Pumped thermal electricity storage: a technology overview”. In: *Thermal Science and Engineering Progress* 6 (2018), pp. 301–315.
[5] Olivier Dumont et al. “Carnot battery technology: A state-of-the-art review”. In: *Journal of Energy Storage* 32 (2020), p. 101756.
[6] Andrea Vecchi et al. “Carnot Battery development: A review on system performance, applications and commercial state-of-the-art”. In: *Journal of Energy Storage* 55 (2022), p. 105782.
[7] Alberto Benato and Anna Stoppato. “Energy and cost analysis of a new packed bed pumped thermal electricity storage unit”. In: *Journal of Energy Resources Technology* 140.2 (2018), p. 020904.
[8] Alberto Benato and Anna Stoppato. “Integrated thermal electricity storage system: energetic and cost performance”. In: *Energy conversion and management* 197 (2019), p. 111833.
[9] Tristan Desrues et al. “A thermal energy storage process for large scale electric applications”. In: *Applied Thermal Engineering* 30.5 (2010), pp. 425–432.
[10] Alberto Benato et al. “TES-PD: A fast and reliable numerical model to predict the performance of thermal reservoir for electricity energy storage units”. In: *Fluids* 6.7 (2021), p. 256.
[11] Lorenzo Pilotti, Alessandro Francesco Castelli, and Emanuele Martelli. “Optimal design of fully renewable and dispatchable power plants with hydrogen seasonal storage”. In: *Renewable Energy* 241 (2025), p. 122195.
[12] Tiberio Puri et al. “AN INNOVATIVE TOOL FOR OPTIMIZING THE ENERGY HUB OF LARGE BUILDINGS: THE CASE STUDY OF A NEW HOSPITAL IN NORTHERN ITALY”. In: *ECOS 2025*. 2025.
[13] Gurobi Optimization, LLC. *Gurobi Optimization: Decision Intelligence Technology*. 2026.
[14] Rodun International. *Therminol 68 - Fluido de transferencia de calor*. Accesso: 24 marzo 2026. 2026.
[15] European Commission, Joint Research Centre. *Photovoltaic Geographical Information System (PVGIS)*. Accesso: 24 marzo 2024. 2024.
[16] Gestore dei Mercati Energetici S.p.A. *GME - Mercato Elettrico*. Accesso: 24 marzo 2024. 2024.
[17] Stefano Campanari, Ennio Macchi, Paolo Silva, et al. *La micro-cogenerazione a gas naturale*. Polipress, 2005.
[18] Matteo Pecchini et al. “Analysis of the discharge process of a TES-based electricity storage system”. In: *Journal of Energy Storage* 100 (2024), p. 113518.
[19] Simone Peccolo et al. “A novel design approach for Carnot Batteries thermal energy storage tank”. In: *Energy Conversion and Management* 346 (2025), p. 120405.